OPEN ACCESS Freely available online

PLOS ONE

Mechanistic Study of Manganese-Substituted Glycerol Dehydrogenase Using a Kinetic and Thermodynamic Analysis

Baishan Fang[1,2], Jin Niu[1], Hong Ren[1], Yingxia Guo[1], Shizhen Wang[1,2]*

1 Department of Chemical and Biochemical Engineering, College of Chemistry and Chemical Engineering, Xiamen University, Xiamen, China, **2** The Key Lab for Synthetic Biotechnology of Xiamen City, Xiamen University, Xiamen, China

Abstract

Mechanistic insights regarding the activity enhancement of dehydrogenase by metal ion substitution were investigated by a simple method using a kinetic and thermodynamic analysis. By profiling the binding energy of both the substrate and product, the metal ion's role in catalysis enhancement was revealed. Glycerol dehydrogenase (GDH) from *Klebsiella pneumoniae* sp., which demonstrated an improvement in activity by the substitution of a zinc ion with a manganese ion, was used as a model for the mechanistic study of metal ion substitution. A kinetic model based on an ordered Bi-Bi mechanism was proposed considering the noncompetitive product inhibition of dihydroxyacetone (DHA) and the competitive product inhibition of NADH. By obtaining preliminary kinetic parameters of substrate and product inhibition, the number of estimated parameters was reduced from 10 to 4 for a nonlinear regression-based kinetic parameter estimation. The simulated values of time-concentration curves fit the experimental values well, with an average relative error of 11.5% and 12.7% for Mn-GDH and GDH, respectively. A comparison of the binding energy of enzyme ternary complex for Mn-GDH and GDH derived from kinetic parameters indicated that metal ion substitution accelerated the release of dioxyacetone. The metal ion's role in catalysis enhancement was explicated.

Citation: Fang B, Niu J, Ren H, Guo Y, Wang S (2014) Mechanistic Study of Manganese-Substituted Glycerol Dehydrogenase Using a Kinetic and Thermodynamic Analysis. PLoS ONE 9(6): e99162. doi:10.1371/journal.pone.0099162

Editor: Joel H. Weiner, University of Alberta, Canada

Received February 27, 2014; **Accepted** May 12, 2014; **Published** June 4, 2014

Funding: This work was supported by the National Natural Science Foundation of China (No. 41176111, No. 41306124), the Key Program of National Natural Science Foundation of China (No. 21336009), the Natural Science Foundation of Fujian Province of China (No. 2012J01049), and the Fundamental Research Funds for the Central Universities (No. 2013121029). The funders had no role in study design, data collection and analysis, decision to publish, or preparation of the manuscript.

Competing Interests: The authors have declared that no competing interests exist.

* E-mail: szwang@xmu.edu.cn

Introduction

Various metalloenzymes act in fundamental biological processes found in nature. The metal ion of most metalloenzymes participates in the catalytic process involved in the function of the polarization of chemical bonds, nucleophile activation, and substrate or product coordination [1]. Substitution of metal ions in metalloenzymes is a mild and effective modification that is used in structure-function relationship studies [2]. Metal ion substitutions have been reported to change the catalytic activity [3], substrate specificity [4], and stability [5,6] of metalloenzymes and have stimulated much research interest. The mechanism of metal ion substitution has been mainly studied by molecular simulation and the analysis of substituted enzyme crystals. Sparta [7] studied the metal ion substitution effects of catechol-O-Methyltransferase activity by a quantum mechanical/molecular mechanical dynamics method. Metal ion substitution affected the rate-limiting step, which was explicated as the methyl transfer that occurred with a significant increase in the activation barrier. D'Antonio investigated the structure of cobalt-reconstituted human arginase I, revealing the change of the catalytic mechanism upon metal ion substitution [8]. However, the molecular simulation of the enzyme structure and the generation of metal ion substituted enzyme crystals are lengthy and expensive processes.

Compared with dynamic simulation and structure analysis, thermodynamic and kinetic analysis is a simple, quick and valid strategy aimed at explaining the activity and functional properties of biocatalysis systems [9]. The microenvironment of the active site of the metalloenzyme involved in the reaction mechanism undergoes dynamic and structural changes upon metal ion substitution [10]. Free energy binding profiles of substrates and products with modified enzymes and enzyme-substrate complexes, which demonstrate the catalytic requirement for transition state stabilization and ground state stabilization, offer an alternative method for studying the influence of metal ion substitution on catalytic reactions [11]. A kinetic and thermodynamic analysis of each binding step of the substrate and product can be used for profiling the significant changes caused by metal ion substitution and can provide valuable information for further study.

Glycerol dehydrogenases play crucial roles enzymes in the pathway of glycerol metabolism, industrial applications and even pathogenicity [12,13]. The NAD^+-linked GDHs are members of the medium-chain alcohol dehydrogenase family, most of which are metalloenzymes [14]. They dehydrogenate glycerol to dihydroxyacetone and lead to the production of value-added products, namely, DHA, butanol, succinic acid and citric acid [15,16]. GDHs are also widely used for the enzymatic determination of glycerol for medical diagnoses and fermentation process

analyses [17,18]. Coupling with other oxidoreductases, GDH is part of a multi-enzyme system for the biosynthesis of chiral intermediates with cofactor regeneration [19]. Therefore, glycerol dehydrogenase was selected as a model enzyme for this metal ion substitution study.

Glycerol dehydrogenase from *Klebsiella pneumoniae* sp. is a zinc-dependent metalloenzyme [20]. It has been previously shown that Mn^{2+} substituted GDH exhibits improved activity and thermostability [21]. In this paper, mechanistic insights of activity improvement are studied based on kinetic and thermodynamic analysis. A kinetic model based on an ordered Bi-Bi mechanism with substrate and product inhibition is proposed. The equilibrium constants for each ligand-binding are calculated by using the forward and reverse rate constants. By profiling the binding rate and energy for substrate and product with enzyme, the rate accelerating step is determined. The metal ion's role in catalysis enhancement is investigated.

Results and Discussion

The influence of substrate concentration

The influence of substrate concentration of both substrates, NAD^+ and glycerol, on GDH (Fig. 1a) and Mn-GDH (Fig. 1b) were studied. Double reciprocal plots of six NAD^+ concentrations versus reaction rates at six fixed glycerol concentrations were drawn [22]. Earlier studies that were conducted on glycerol dehydrogenase from *Klebsiella pneumonia* [23] and from other microorganisms [24,25] reported the GDHs follow an ordered Bi-Bi sequential mechanism. Therefore, it was reasonable to assume that GDH from *Klebsiella pneumonia* and Mn-GDH obey the ordered Bi-Bi sequential mechanism. Kinetic parameters were determined from Lineweaver-Burke plots. The kinetic parameters for GDH and Mn-GDH are listed in Table 1.

The influence of product concentration

The product inhibition of Mn-GDH was studied by varying the concentration of each product, DHA (0–0.40 mmol/L) and NADH (0–0.20 mmol/L). NADH competitively inhibited the enzyme at a constant concentration of glycerol (Fig. 2a), which was consistent with a compulsory ordered Bi-Bi reaction mechanism. The inhibition constant of NADH, K_{iQ}, which was derived by secondary plots (Fig.2b) of the slopes determined from the primary double-reciprocal plots [22] against each fixed NADH concentration, was calculated as 0.02 mmol/L.

DHA inhibited the enzyme noncompetitively with respect to NAD^+ at a constant concentration of glycerol (Fig. 3a). The inhibition constant of DHA, K_{iP}, derived by secondary plots of the slopes determined from the primary double-reciprocal plots (Fig.3b), was calculated as 0.52 mmol/L. Product inhibition indicated that Mn-GDH obeyed a compulsory ordered-Bi-Bi mechanism. The inhibition constant of DHA and NADH for GDH were calculated. K_{iP}, and K_{iQ} were 0.45 mmoL/L and 0.015 mmoL/L, respectively.

Kinetic model development

An ordered Bi-Bi mechanism kinetic model was proposed. The King-Altman plot of this model is shown in Fig. 4. In this model, NAD^+ (A) binds first to the free enzyme (E). The second substrate, glycerol, binds subsequently, forming the ternary complex (EAB). Upon isomerization, the product-bound complex (EPQ) is formed. After the release of the first product, DHA (P), the second product, NADH (Q), dissociates, leaving the free enzyme.

The corresponding volumetric rate of NADH, derived from King-Altman method and transformed using Cleland's coefficient form, is given by Eq.1.

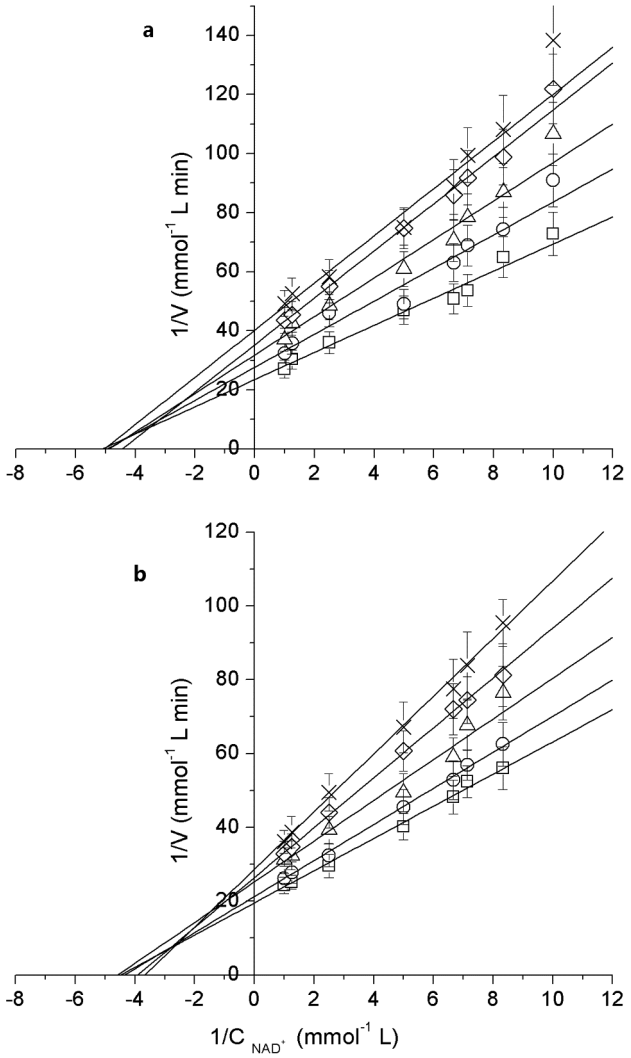

Figure 1. The influence of glycerol concentration. a. The influence of glycerol concentration for GDH; b. The influence of glycerol concentration for Mn-GDH. Reaction conditions: Glycerol concentration (×: 0.010 mol/L, 0.015 mol/L, Δ: 0.025 mol/L, O: 0.100 mol/L, □: 0.200 mol/L); enzyme, 1 mg/L; pH 12.0; temperature, 45°C.
doi:10.1371/journal.pone.0099162.g001

$$v_{\mathrm{NADH}}=\frac{V^f V^r([A][B]-\frac{[P][Q]}{K_{eq}})}{V^r K_{iA}Km_B+V^r Km_B[A]+V^r Km_A[B]+V^r[A][B]+\frac{V^r Km_A[B][Q]}{K_{iQ}}+\frac{V^r[A][B][P]}{K_{iP}}+\frac{V^f}{K_{eq}}Km_Q[P]+\frac{V^f}{K_{eq}}Km_P[Q]+\frac{V^f}{K_{eq}}[P][Q]+\frac{V^f Km_Q[A][P]}{K_{eq}K_{iA}}+\frac{V^f[B][P][Q]}{K_{eq}K_{iB}}} \quad (1)$$

Eq.2 and Eq.3, which describe the relevance between kinetic constants, were obtained by applying Haldane equations. K_{eq} and K_{iB} were replaced with Eq.2, Eq.3, respectively. The value of K_{mA}, K_{mB}, K_{iA}, K_{iP} and K_{iQ} were derived from the above experiments.

$$K_{eq}=\frac{V^f K_{mP}K_{iQ}}{V^r K_{mB}K_{iA}} \quad (2)$$

$$K_{iB}=\left(\frac{V^f}{V^r}\right)^2\frac{K_{mQ}K_{iP}}{Km_A K_{eq}} \quad (3)$$

Table 1. Kinetic parameters of Mn-GDH and GDH.

Kinetic parameters	Mn-GDH	GDH
K_{mA}* (mmol/L)	0.008±0.001	0.005±0.001
K_{mB}*(mmol/L)	0.226±0.013	0.262±0.014
K_{iA} (mmol/L)	0. 012±0.002	0.008±0.001

*K_{mA}, the Michaelis-Menten constant of NAD^+; K_{mB}, the Michaelis-Menten constant of glycerol.
Reaction conditions: Glycerol concentration (0.010–0.400 mmol/L); enzyme, 1 mg/L; pH 12.0; temperature, 45°C.
doi:10.1371/journal.pone.0099162.t001

Parameter estimation

The values of the kinetic parameters, namely K_{mA}, K_{mB}, K_{iA}, K_{iB}, K_{iP}, K_{iQ}, was obtained previously, which were used for the final parameter estimation via nonlinear regression [26]. K_{eq} is a dependent parameter. Therefore, the number of estimated parameters was reduced from 10 to 4. Kinetic parameters for estimation can be remarkably decreased. The concentration-time curve data with various substrate concentrations were used for the simulation of the remaining four parameters, namely, V^f, V^r, K_{mP},

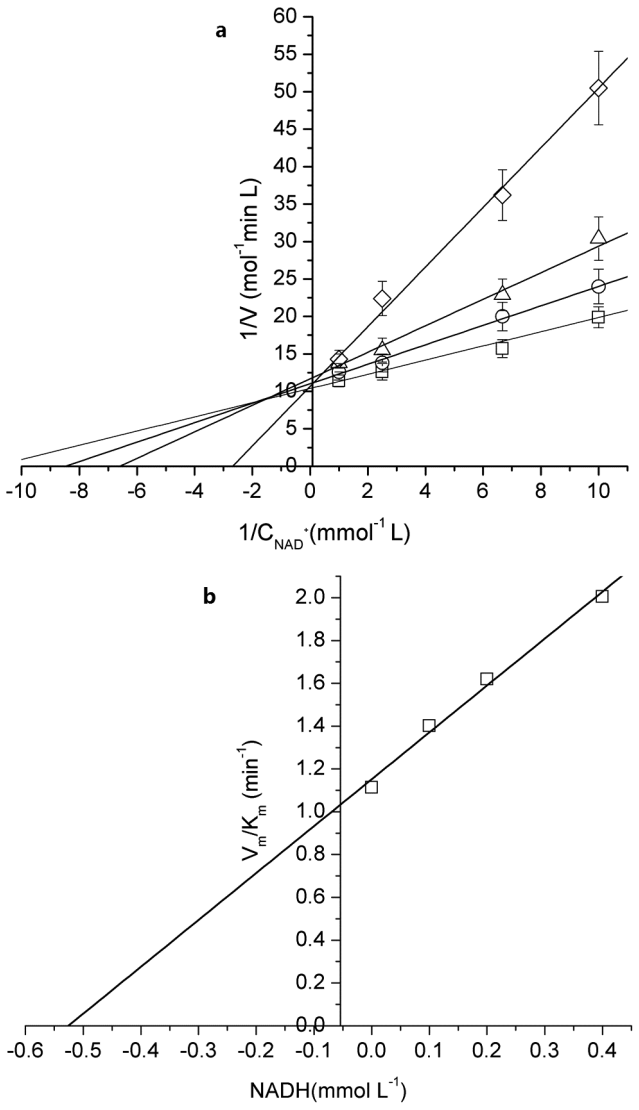

Figure 2. Product inhibition of NADH for Mn-GDH. a. Double reciprocal plots of NADH concentrations versus reaction rates b. The secondary plots of the slopes for product inhibition of NADH for Mn-GDH. Reaction conditions: NADH concentration (□: 0 mmol/L, O: 0.05 mmol/L, Δ: 0.10 mmol/L, ◇: 0.20 mmol/L); glycerol 0.40 mol/L; Mn-GDH, 1 mg/L; pH 12.0; temperature, 45°C.
doi:10.1371/journal.pone.0099162.g002

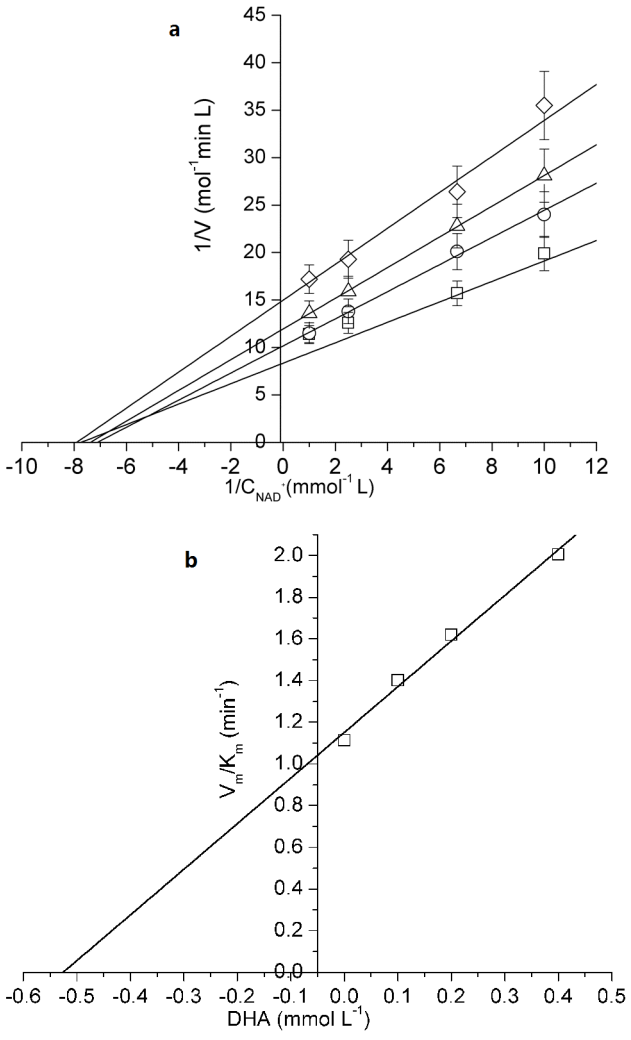

Figure 3. Product inhibition of DHA for Mn-GDH. a. Double reciprocal plots of NADH concentrations versus reaction rates. b. The secondary plots of the slopes for product inhibition of DHA for Mn-GDH. Reaction conditions: DHA (□: 0 mmol/L, O: 0.10 mmol/L, Δ: 0.20 mmol/L, ◇: 0.40 mmol/L); glycerol 0.40 mol/L; Mn-GDH, 1 mg/L; pH 12.0; temperature, 45°C.
doi:10.1371/journal.pone.0099162.g003

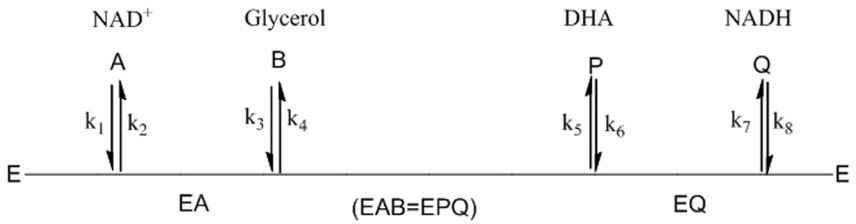

Figure 4. Compulsory ordered Bi-Bi reaction mechanism.
doi:10.1371/journal.pone.0099162.g004

and K_{mQ}, by the MATLAB program. Parameter estimation was carried out by a combination of fourth- and fifth-order Runge kutta method using ode45 module in MATLAB software. All datasets were fitted at once. These parameters are listed in Table 2. The comparisons of simulated values with the experimental data for Mn-GDH and GDH are shown in Fig. 5 and Fig. 6. There was a good agreement between the experimental and simulated values, with 11.5% and 12.7% average relative error for Mn-GDH and GDH, respectively.

Thermodynamic study

The thermodynamic parameters, which are highly complex and interdependent, can be derived from kinetic parameters. Most ligand-binding reactions are studied by calculating the values of the binding equilibrium constant and binding energy of each step [11]. Parameters for each step provide further insights into the binding process, which reveals the effect of metal ion substitution.

The rate constants for each binding step (k_1-k_8), which are shown in Table 3, were calculated according to the definition of rate constants in terms of kinetic constants [22]. K_{EA}, K_{EAB}, K_{EPQ} and K_{EQ} were assigned as the equilibrium constants for each ligand-binding event [11]. The binding equilibrium constants are listed in Table 4. The Mn-GDH and GDH have nearly the same K_{EAB} value, while a higher K_{EPQ} value for Mn-GDH.

Binding energy of the enzyme ternary complex EPQ (enzyme-DHA-NADH complex), which were defined as -RTlnK_{EPQ}, for Mn-GDH and GDH were 1.95 and 3.18 KJ/mol, respectively. This revealed that the substitution of manganese mainly depended on accelerating the release of dioxyacetone [27,28].

Manganese has the similarity with the other divalent cations, which are Lewis acids and electrostatic stabilizers. Manganese can be replaceable with other metals, namely, magnesium and zinc. This depends on the intermediate properties of Mn^{2+} relative to these other ions, including its radius length and borderline hard–soft character [29]. Metal ions with important biological function can be classified as hard and soft, while hard acids and bases are weak polar, have small ionic radius and high oxidation state. The soft species are on the contrary [30]. Replacing the catalytic zinc with manganese revealed electronic requirements for the specific geometry of the catalytic site of GDH.

Conclusion

A simple, quick and valid strategy based on kinetic and thermodynamic analysis for understanding the significant mechanistic changes induced by metal ion substitution was proposed. By profiling the binding rate and energy for the substrate and product of the enzyme, the rate accelerating step was determined. The mechanism of increasing the catalytic activity of glycerol dehydrogenase by manganese substitution was studied. A kinetic model based on the ordered Bi-Bi mechanism with both product and substrate inhibition was proposed. Further mechanistic insights regarding the role of the metal ion in catalysis enhancement were investigated by characterizing the binding kinetics and thermodynamics of each step. The kinetic parameters were simulated by the MATLAB program. The thermodynamic

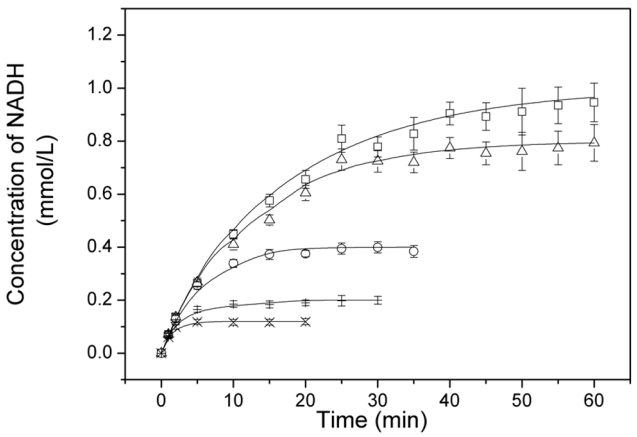

Figure 5. Comparison of the simulated values with the experimental data for Mn-GDH reaction conditions: NAD^+ (□: 1.0 mmol/L; Δ: 0.8 mmol/L, O: 0.4 mmol/L, +: 0.2 mmol/L, ×: 0.12 mmol/L), simulated (lines, —); glycerol, 0.1 mol/L; Mn-GDH, 1 mg/L; pH, 12.0; temperature, 45°C.
doi:10.1371/journal.pone.0099162.g005

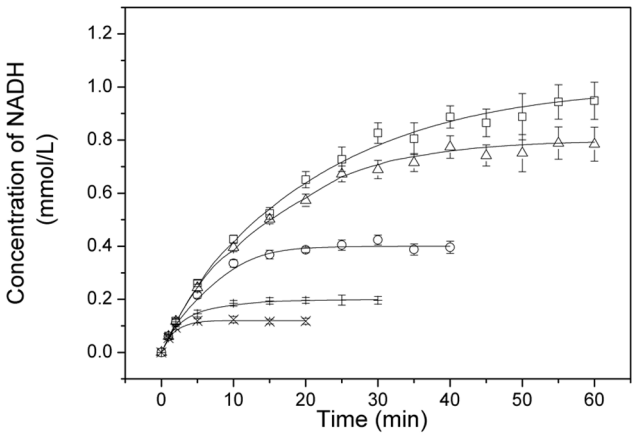

Figure 6. Comparison of the simulated values with the experimental data for GDH. reaction conditions: NAD^+ (□: 1.0 mmol/L; Δ: 0.8 mmol/L, O: 0.4 mmol/L, +: 0.2 mmol/L, ×: 0.12 mmol/L), simulated (lines, —); glycerol, 0.1 mol/L; GDH, 1 mg/L; pH, 12.0; temperature, 45°C.
doi:10.1371/journal.pone.0099162.g006

Table 2. Estimated values of kinetic parameters.

Kinetic parameters	Mn-GDH	GDH
V^f (mmol/L/min)	0.080	0.068
V^r (mmol/L/min)	0.0104	0.0074
K_{mA}*(mmol/L)	0.008	0.262
K_{mB}* (mmol/L)	0.005	0.226
K_{iA}* (mmol/L)	0.012	0.008
K_{iB}** (mmol/L)	0.301	0.66
K_{mP} (mmol/L)	0.451	0.28
K_{mQ} (mmol/L)	0.002	0.0016
K_{ip}* (mmol/L)	0.52	0.45
K_{iQ}* (mmol/L)	0.02	0.015
K_{eq}**	25.6	18.4

*: the fixed parameters.
**: the dependent parameters.
doi:10.1371/journal.pone.0099162.t002

parameters were derived from the kinetic parameters, which indicated that the metal ion substitution facilitated the release of dioxyacetone.

The kinetic and thermodynamic analysis contributed further insights regarding the prediction and optimization of polyol dehydrogenases that are widely used for chiral alcohol production. This study also provided valuable information for further investigation by molecular simulation. Metal coordination is a key structural and functional component of enzyme. Given this dual role, metal coordination plays a template role in folded and functional protein domains and complexes. The study of metal ions coordination effect based on kinetic and thermodynamic study will provided a promising method metal induced multi-enzyme assembly study [31].

Materials and Methods

Materials

Glycerol, NAD^+, NADH, and ethylenediaminetetraacetic acid (EDTA) were purchased from Sigma Chem. Co. (Beijing, China). The media (Tryptone, yeast extract, nutrient broth) were purchased from Sangon Biotech Co. Ltd. (Shanghai, China). All other chemicals used were analytical grade and were purchased from either Sigma or Merck (Beijing, China).

Table 3. The rate constants.

Rate constants	Mn-GDH	GDH
k_1 (L/min/mmol)	10000	13600
k_2 (/min)	120	109
k_3 (L/min/mmol)	366	260
k_4 (/min)	11	8
k_5 (/min)	347	3431
k_6 (L/min/mmol)	725	11446
k_7 (/min)	104	69
k_8 (L/min/mmol)	5200	4625

doi:10.1371/journal.pone.0099162.t003

Preparation of the apoenzyme and metal substitution

The preparation of purified GDH followed a previously published method [19]. Recombinant GDH was expressed by transforming plasmids containing the *gld*A gene (GenBank: AKAM01000021.1), which codes for glycerol dehydrogenase, into *E. coli* BL21 (DE3). Metal substitution was accomplished using purified GDH using the following steps: chelation of GDH's catalytic zinc ion using EDTA (1.0 mmol/L) for 4 h at 28°C and removal of EDTA-Zn^{2+} from the GDH solution by dialysis in binding buffer (pH 7.4, changed every 8 h) at 4°C for 53 h. The manganese ion was introduced by the co-incubation of the GDH apoenzyme with $MnCl_2$ (10.0 mmol/L) for 1 h at 37°C. A reference experiment was performed by directly adding Mn^{2+} (10 mmol/L) to native GDH to investigate the activation effects of bivalent ions. The results indicated that the addition of Mn^{2+} to the reaction solution decreased the activity of GDH. The activity of the apoenzyme after EDTA treatment was nearly undetectable, which confirmed the activity enhancement by metal ion substitution [21].

Enzyme assay and kinetic study

The activity of glycerol dehydrogenase was measured by following the increase of NADH concentration using a Spectra Max M5 Microplate Reader (California, United States). Measurements were taken at 340 nm, and a molar extinction coefficient of 6.22/mM/cm was used. One unit of GDH activity was defined as the amount of enzyme necessary to oxidize 1 μmol of NADH per minute under the following conditions (45°C,

Table 4. The binding equilibrium constants of enzyme-substrate complex.

Binding equilibrium constants	Mn-GDH	GDH
K_{EA}	0.012	0.008
K_{EAB}	0.030	0.030
K_{EPQ}	0.48	0.30
K_{EQ}	0.02	0.015

doi:10.1371/journal.pone.0099162.t004

0.1 mol/L potassium carbonate buffer, pH 12.0). The assay mixture contained 0.4 mol/L glycerol, 0.1–1.0 mmol/L NAD^+, and 0.1 mol/L potassium carbonate buffer (pH 12.0). The volume of the reaction mixture was 200 μL in all cases. Reactions were started by the addition of the enzyme solution. Enzyme activities were determined in triplicate. Three blank controls were used as a reaction mixture with the apoenzyme, without the enzyme, and without NAD^+. For the product inhibition study, the reactions were carried out with different DHA or NADH concentrations.

Author Contributions

Conceived and designed the experiments: SZW BSF. Performed the experiments: JN HR YXG. Wrote the paper: SZW. Read and approved the final manuscript: BSF JN HR YXG SZW.

References

1. Andreini C, Bertini I, Cavallaro G, Holliday GL, Thornton JM (2008) Metal ions in biological catalysis: from enzyme databases to general principles. J Biol Inorg Chem 13: 1205–1218.
2. Kleifeld O, Frenkel A, Martin JML, Sagi I (2003) Active site electronic structure and dynamics during metalloenzyme catalysis. Nat Struct Biol 10: 98–103.
3. Cappiello M, Alterio V, Amodeo P, Del Corso A, Scaloni A, et al. (2006) Metal ion substitution in the catalytic site greatly affects the binding of sulfhydryl-containing compounds to leucyl aminopeptidase. Biochem 45: 3226–3234.
4. Arima J, Uesugi Y, Hatanaka T (2009) Bacillus D-stereospecific metallo-amidohydrolase: Active-site metal-ion substitution changes substrate specificity. Biochim 91: 568–576.
5. Bogin O, Peretz M, Burstein Y (1997) *Thermoanaerobacter brockii* alcohol dehydrogenase: Characterization of the active site metal and its ligand amino acids. Protein Sci 6: 450–458.
6. Rochu D, Viguie N, Renault F, Crouzier D, Froment MT, et al. (2004) Contribution of the active-site metal cation to the catalytic activity and to the conformational stability of phosphotriesterase: temperature- and pH-dependence. Biochem J 380: 627–633.
7. Sparta M, Alexandrova AN (2012) How metal substitution affects the enzymatic activity of catechol-O-nethyltransferase. PLoS ONE 10: e47172.
8. D'Antonio EL, Christianson DW (2011) Crystal structures of complexes with cobalt-reconstituted human arginase I. Biochemistry 50: 8018–8027.
9. Alberty RA (2010) Biochemical thermodynamics and rapid-equilibrium enzyme kinetics. J Phys Chem B 114: 17003–17012.
10. Bohacek RS, McMartin C (1994) Multiple highly diverse structures complementary to enzyme binding sites: results of extensive application of a de Novo design method incorporating combinatorial growth. J Am Chem Soc 116: 5560–5571.
11. Fisher HF (2010) Protein–ligand interactions: thermodynamic basis and mechanistic consequences. Encyclopedia of life sciences, 1–10. DOI: 10.1002/9780470015902.a0001341.pub
12. Wang Y, Tao F, Xu P (2014) Glycerol dehydrogenase plays a dual role in glycerol metabolism and 2, 3-butanediol formation in *Klebsiella pneumoniae*. J Biol Chem. 113: 525–535.
13. Zhang K, Zhao WD, Li Q, Fang WG, Zhu L, et al. (2009) Tentative identification of glycerol dehydrogenase as *Escherichia coli* K1 virulence factor cglD and its involvement in the pathogenesis of experimental neonatal meningitis. Med. Microbiol. Immunol. 198, 195–204
14. Ruzheinikov SN, Burke J, Sedelnikova S, Baker PJ, Taylor R, et al. (2001) Glycerol dehydrogenase: Structure, specificity, and mechanism of a family III polyol dehydrogenase. Structure 9: 789–802.
15. Dobson R, Gray V, Rumbold K (2012) Microbial utilization of crude glycerol for the production of value-added products. J Ind Microbiol Biotechnol 39: 217–226.
16. Enders D, Voith M, Lenzen A (2005) The dihydroxyacetone unit - A versatile C-3 building block in organic synthesis. Angew Chem Int Ed 44: 1304–1325.
17. Sokic-Lazic D, Arechederra RL, Treu BL, Minteer SD (2010) Oxidation of biofuels: fuel diversity and effectiveness of fuel oxidation through multiple enzyme cascades. Electroanal 22: 757–764.
18. Lapenaite I, Ramanaviciene A, Ramanavicius A (2006) Current trends in enzymatic determination of glycerol. Crit Rev in Anal Chem 36: 13–25.
19. Zhang Y, Gao F, Zhang SP, Su ZG, Ma GH, et al. (2011) Simultaneous production of 1,3-dihydroxyacetone and xylitol from glycerol and xylose using a nanoparticle-supported multi-enzyme system with in situ cofactor regeneration. Bioresource Technol 102: 1837–1843.
20. Tang JCT, Forage RG, Lin ECC (1982) Immunochemical properties of NAD^+-linked glycerol dehydrogenases from *Escherichia coli* and *Klebsiella pneumonia*. J Bacteriol 152: 1169–1174.
21. Wang SZ, Wang J, Zhou XF, Guo YX, Fang BS (2013) The improvement of stability, activity and substrate promiscuity of glycerol dehydrogenase substituted by divalent metal ions. Biotechnol Bioproc E 18: 796–800.
22. Leskovac V (2004) Comprehensive enzyme kinetics. NewYorkKluwer Academic/Plenum Publishers, 141–147.
23. Chen HW, Nie JF, Chen G, Fang BS (2010) Kinetic mechanisms of glycerol dehydrogenase and 1,3-propanediol oxidoreductase from *Klebsiella pneumonia*. Chin J Biotech 26: 177–182.
24. Zheng MQ, Zhang SP (2011) Immobilization of glycerol dehydrogenase on magnetic silica nanoparticles for conversion of glycerol to value-added 1,3-dihydroxyacetone. Biocatal Biotransfor 29: 278–287.
25. Nishise H, Nagao A, Tani Y, Yamada H (1984) Further characterization of glycerol dehydrogenase from *Cellulomonas* sp. NT3060. Agr Biol Chem 48: 1603–1609.
26. Chen BH, Hibbert EG, Dalby PA, Woodley JM (2008) A new approach to bioconversion reaction kinetic parameter identification. AIChE J 54: 2155–2163.
27. Siddiqui KS, Cavicchioli R (2006) Cold-adapted enzymes. Annu Rev Biochem 75: 403–433.
28. Fisher HF (2001) Protein ligand interactions: Molecular basis. Encyclopedia of life sciences, 1–9 DOI:10.1038/npg.els.0001341.
29. Martinez-Rodriguez S, Encinar JA, Hurtado-Gomez E, Prieto J, Clemente-Jimenez JM, et al. (2009) Metal-triggered changes in the stability and secondary structure of a tetrameric dihydropyrimidinase: A biophysical characterization. Biophys Chem 139: 42–52.
30. Lemire JA, Harrison JJ, Turner RJ (2013) Antimicrobial activity of metals: mechanisms, molecular targets and applications. Nat Rev Microbiol 11: 371–384.
31. Salgado EN, Ambroggio XI, Brodin JD, Lewis RA, Kuhlman B, et al. (2010) Metal templated design of protein interfaces. P Natl Acad Sci USA 107: 1827–1832.